JOURNAL OF OPTOELECTRONICS AND ADVANCED MATERIALS Vol. 12, No. 8, August 2010, p. 1706 - 1713

Calorimetric studies of $(Se_{80}Te_{20})_{100-x}Ag_x$ bulk samples

D. SINGH, S. KUMAR, R. THANGARAJ*
Semiconductors Laboratory, Department of Physics, Guru Nanak Dev University, Amritsar-143005, Punjab, India

The crystallization kinetics of bulk amorphous $(Se_{80}Te_{20})_{100-x}Ag_x$ ($0 \le x \le 4$) glasses has been carried out using Differential Scanning Calorimetry at different heating rates (5-20 K/min) under non-isothermal conditions. It is found that the glass transition temperature and the crystallization temperature decrease with increase in Ag content. The apparent activation energy for glass transition and the activation energy for crystallization have been determined using the Moynihan's relation, modified Kissinger and Matusita equations.

(Received July 2, 2010; accepted August 12, 2010)

Keywords: Crystallization, DSC, Calorimetric

1. Introduction

Chalcogenide glasses are based on the chalcogen elements S, Se and Te but not O. The chalcogenide glasses are some of the widely used amorphous semiconductors for a variety of applications in optics, optoelectronics, waveguides, optical memories, infrared lasers etc. There has been an increased interest in the properties of Se-rich chalcogenide glassy alloys due to their current use as photoreceptors in TV vidicon pickup tubes [1] and in digital X-ray imaging [2]. Selenium is considered to be one of the most important semiconductors due to its unusual structure [3] and it exhibits the unique property of reversible phase transformation [4]. It has the wide commercial applications like switching, memory and xerography which make it attractive. But in the pure state it has the disadvantages of short lifetime and low sensitivity and low thermal instability. This problem can be removed by alloying Se with some impurity atoms which gives higher sensitivity, higher crystallization temperature and smaller ageing effects [5-7]. It has been pointed out that addition of Te to Se improves the corrosion resistance [8] and lengthens the crystallization time of amorphous selenium [9]. Glassy alloys of the Se-Te system based on selenium have become materials of considerable commercial importance and are widely used for optical recording media because of their excellent laser writing sensitivity [10] but these advantages depend on material stability [11]. The Se-Te alloys have been found to be useful from the technological point of view due to their greater hardness, higher crystallization temperature T_C, and smaller ageing effects as compared to a-Se [12]. Experimental results indicate that the properties of the Se-Te alloys are highly composition dependent. Addition of Ag will expand the glass forming area and also create compositional and configurational disorder in the system and has large effect on their structural, physical, optical, electronic and thermal properties [13]. In the present work, the activation energy of glass transition and crystallization of $(Se_{80}Te_{20})_{100-x}Ag_x$ glass has been discussed based on characteristic temperatures such as the glass transition temperature (T_g) and the crystallization temperature (T_c). Theoretical models [14–16] were applied to calculate crystallization kinetics for the crystallization process under non-isothermal conditions.

2. Experimental

Bulk samples of $(Se_{80}Te_{20})_{100-x}Ag_x$ ($0 \le x \le 4$) were prepared by conventional melt quenching technique. High-purity (99.999%) elements with appropriate atomic percentage were sealed in a quartz ampoule (length ~100mm and internal diameter ~6mm) in a vacuum of 10^{-5} mbar. The ampoules were kept inside a vertical furnace for 72 h. The temperature was raised to 1373K, at a rate of 4-5 K/min. The ampoule was inverted at regular intervals of time to ensure homogeneous mixing of the constituents. The ampoule was then quenched in ice-cold water. The bulk material was separated from the quartz ampoule by dissolving the ampoule in $HF+H_2O_2$ solution for approximately 48 h. The amorphous nature of the bulk samples was confirmed by the absence of sharp peaks in the X-ray diffractogram. XRD studies were done using Phillips PAN ANALYTICAL machine and X-ray of Cu K_α line to check the amorphous nature of the materials. About one gram of bulk samples of $(Se_{80}Te_{20})_{100-x}Ag_x$ ($1 \le x \le 4$) have been annealed at 348K and 398K at heating rate of 4-5K/min in the vacuum of 10^{-5} mbar to know about the evolution of different crystalline phases in the material. The thermal behaviour of the samples was investigated using Perkin Elmer (Pyris Diamond) DSC System. In each study approximately 10 mg of the bulk material was used. DSC runs were taken for four different

heating rates i.e., 5, 10, 15 and 20 K/min for each of the composition so as to get glass transition temperature (T_g), crystallization temperature (T_c), peak crystallization temperature (T_p) and melting temperature (T_m). The fraction X_c crystallized at a temperature T was calculated using the relation $X_c = A_T/A$ where A is the total area of the exotherm between T_c and the temperature at which crystallization is completed, A_T is the area between T_c and T. The deconvolution of the broad exothermic peaks was carried out by using the peakFit v4.12 (SeaSolve, USA) software program. The DSC data for the exothermic peak was well fitted by using the Savitzky-Golay algorithm.

3. Results

Fig. 1 shows DSC traces for $(Se_{80}Te_{20})_{100-x}Ag_x$ (x=2) glass at different heating rates. The figure shows only one glass transition temperature (T_g) and one exothermic crystallization peak but two endothermic melting peaks. The presence of two peaks means that there are two phases with melting temperatures represented as T_{m1} and T_{m2}. It can also be seen from Fig. 1 that T_g shifts towards higher temperature with increase in the heating rate. Samples with different x values show similar behaviour. Fig. 2 shows DSC thermograms of samples with various x values at a heating rate of 10K/min. In this system the glass transition temperature is found to decrease with the increase in Ag content (Fig. 2). The exothermic peaks on deconvolution gives two crystallization temperatures (T_{c1} and T_{c2}) and two peak crystallization temperatures (T_{p1} and T_{p2}) corresponding to the first and second peaks respectively. The deconvoluted exothermic peaks are shown in Fig. 3. The parameters determined from DSC thermogram are tabulated in Table 1. The analysis of XRD results, using JCPDS database (1998), reveals the formation of crystalline phases in number of annealed bulk samples. Fig. 4 and Fig. 5 represent the XRD pattern of bulk samples annealed at 348K and 398K for 12 hours respectively. The bulk samples annealed at 348K show the presence of Se_8 phase but the samples annealed at 398K show the presence two phases; Se_8 phase and αAg_5Te_3 phase. However, XRD pattern of bulk samples indicates the formation of αAg_5Te_3. This phase probably gives the peak at 294° C in DSC run [17-18].

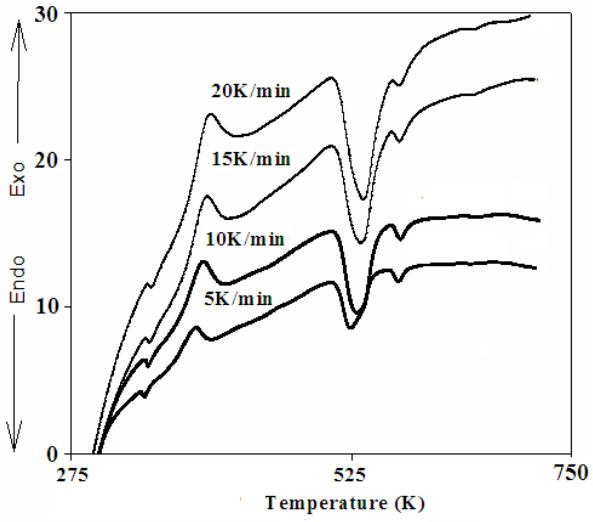

Fig. 1 DSC traces for $(Se_{80}Te_{20})_{100-x}Ag_x$ (x=2) glass at different heating rates.

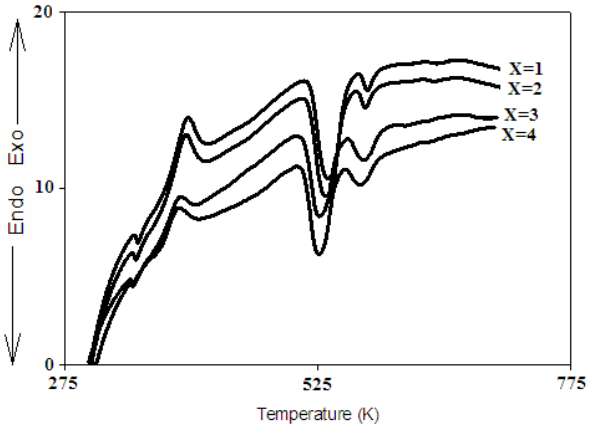

Fig. 2. DSC traces for $(Se_{80}Te_{20})_{100-x}Ag_x$ (0<x<4) glass at heating rate of 10 K/min.

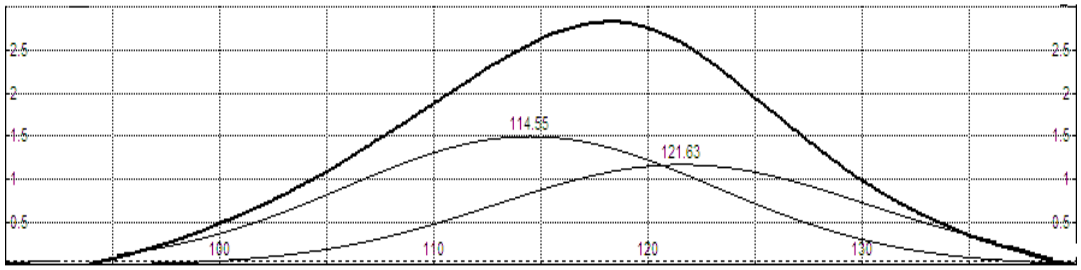

a

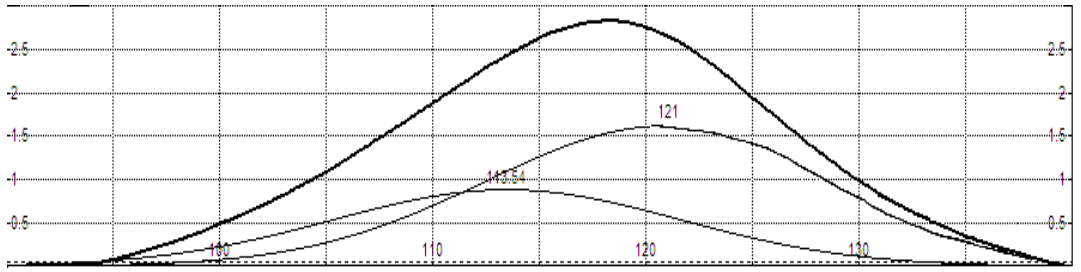

b

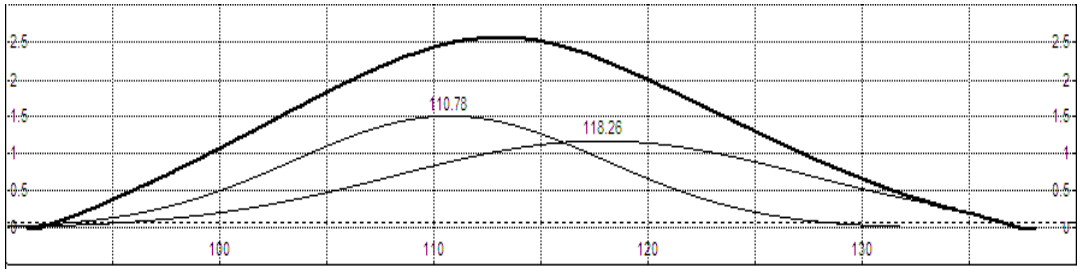

c

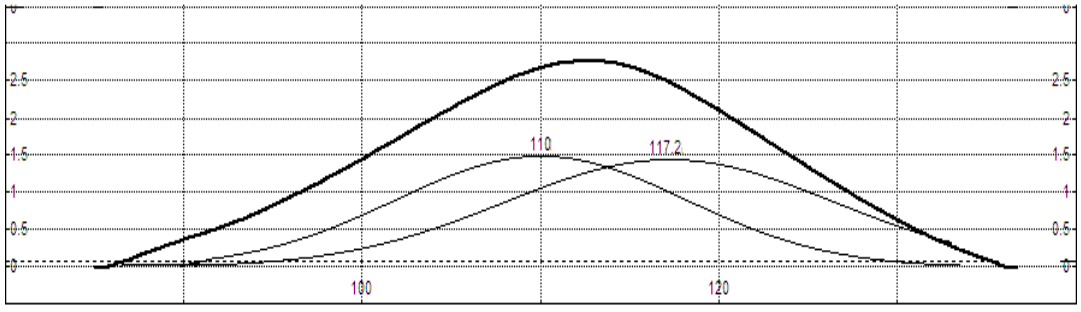

d

Fig. 3 Exothermic peaks before and after deconvolution peak for (a) $(Se_{80}Te_{20})_{99}Ag_1$ (b) $(Se_{80}Te_{20})_{98}Ag_2$ (c) $(Se_{80}Te_{20})_{97}Ag_3$ and (d) $(Se_{80}Te_{20})_{96}Ag_4$ glassy samples. The upper peak shows the best theoretical fit with the simulated base line for the peak while the two deconvoluted exotherms are shown in the lower part. The peak positions at the respective temperatures were also shown in the figure.

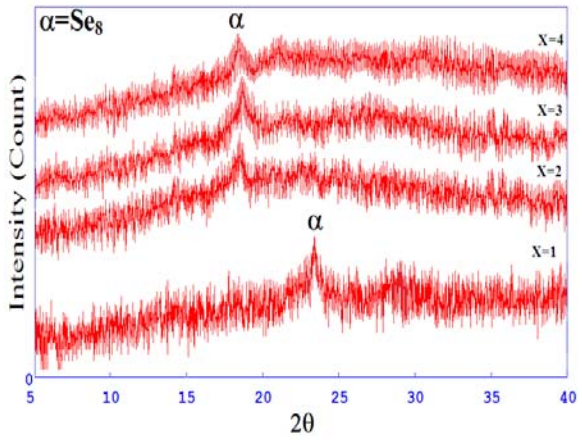

Fig. 4 XRD pattern of $(Se_{80}Te_{20})_{100-x}Ag_x$ (1<x<4) bulk samples annealed at 348K.

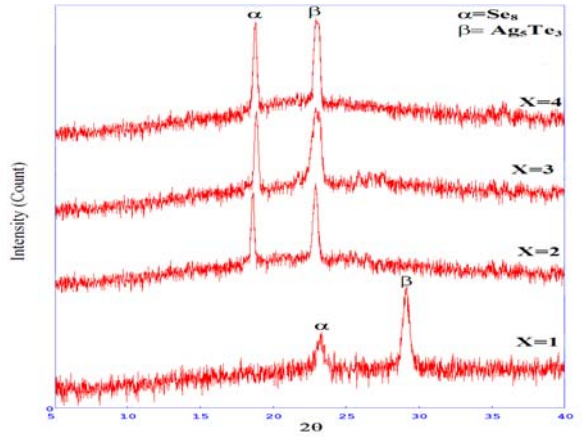

Fig. 5 XRD pattern of $(Se_{80}Te_{20})_{100-x}Ag_x$ (1<x<4) bulk samples annealed at 398K.

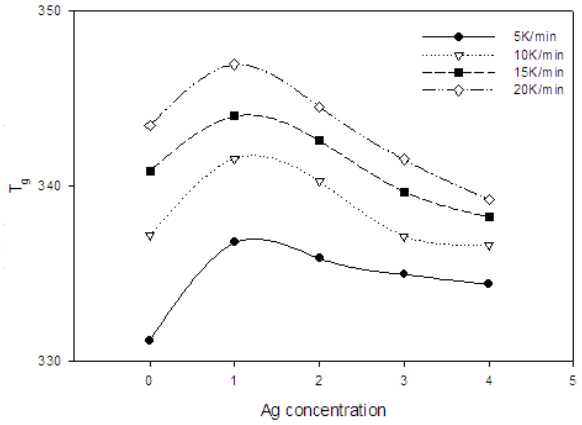

Fig. 6 Plot of T_g with Ag concentration of $(Se_{80}Te_{20})_{100-x}Ag_x$ glassy system at different heating rates.

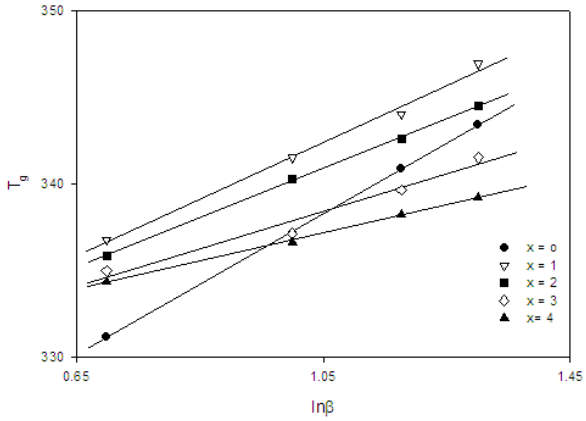

Fig. 7 Plot of T_g with lnβfor $(Se_{80}Te_{20})_{100-x}Ag_x$ glassy system.

The dependence of T_g on heating rate has been analyzed by the two different approaches. The first one is empirical relation of the form

$$T_g = A + B\log\beta$$

where A and B are constants for a given glass composition and β is the heating rate (K/min) employed in DSC runs [21]. The variation in T_g with Ag content is shown in Fig. 6. The value of B is calculated from the slope of T_g vs. lnβ plots (Fig. 7). The value of B is found to vary from 16.594 to 8.08 for different samples (Table 1). The change in B with Ag concentration indicates that $(Se_{80}Te_{20})_{100-x}Ag_x$ alloy undergoes structural changes with Ag addition [19]. The evaluation of apparent activation energy of glass transition using the theory of structural relaxation from the heating rate dependence of glass transition temperature is developed by Moynihan et. al [20-22]. Moynihan's relation is of the form

$$\ln\beta = -\frac{E_t}{RT_g} + const.$$

where R is the gas constant. Plot between lnβ and $1000/T_g$ is a straight line, whose slope yields a value of apparent activation energy E_t (Fig. 8) and their values are listed in Table 1. A linear behaviour has been observed for all the samples. The activation energy for glass transition is found to vary from 58.701 to 124.32 KJ/mol with addition of Ag. The glass activation energy is the amount of energy that is absorbed by a group of atoms in the glassy region so that a jump from one metastable state to another metastable state is possible [23]. In other words, the activation energy is involved in the molecular motions and rearrangements of atoms around the glass transition temperature [24]. Activation energy for crystallization is calculated from the modified Kissinger equation [25, 26]

$$\ln \frac{\alpha^n}{T_p^2} = \frac{-mE_c}{RT_p} + \ln K'$$

where K' is a constant, containing the factors depending on the thermal history of samples, n and m are constants depending upon the morphology of the growth. The slopes of logβ vs. $1000/T_{p1}$ (Fig. 9) and logβ vs. $1000/T_{p2}$ (Fig. 10) yields the values mE_c/n for both phases are shown in Table 2.

Table 1 Parameters determined from DSC thermogram of $(Se_{80}Te_{20})_{100-x}Ag_x$ glassy system taken at 10K/min.

Composition	T_g	T_{c1}	T_{c2}	T_{p1}	T_{p2}	T_{m1}	T_{m2}	B	E_t (KJ/mol)
a-$(Se_{80}Te_{20})_{100}$	337.14	400.3	-	410	-	521	-	16.594	124.32
$(Se_{80}Te_{20})_{99}Ag_1$	341.50	367.59	371.52	387.55	394.63	536	570	16.428	58.701
$(Se_{80}Te_{20})_{98}Ag_2$	340.25	366.42	370.50	386.54	394.00	535	570	14.257	67.365
$(Se_{80}Te_{20})_{97}Ag_3$	337.13	364.60	368.99	383.78	391.26	525	569	10.804	85.207
$(Se_{80}Te_{20})_{96}Ag_4$	336.63	363.82	366.97	383.00	390.20	524	565	8.08	116.458

Table 2 The values of activation energy of crystallization E_c for $(Se_{80}Te_{20})_{100-x}Ag_x$ glassy system obtained by modified Kissinger method and Matusita method taken at 10K/min.

Composition	Peak	mE_c/n(MK) (KJ/mol)	n	m	E_c(MK) (KJ/mol)	mE_c(ME) (KJ/mol)	E_c(ME) (KJ/mol)
a-$(Se_{80}Te_{20})_{100}$	I	97.35	4.05	4	97.35	380.18	95.045
$(Se_{80}Te_{20})_{99}Ag_1$	I	40.5591	2.65	2	40.5591	107.681	53.8405
	II	44.980	2.62	2	44.980	120.479	60.2395
$(Se_{80}Te_{20})_{98}Ag_2$	I	40.7791	2.57	2	40.7791	100.484	50.242
	II	45.1200	2.50	2	45.1200	114.472	57.236
$(Se_{80}Te_{20})_{97}Ag_3$	I	41.7644	2.44	2	41.7644	97.768	48.884
	II	46.7371	2.48	2	46.7371	107.819	53.9095
$(Se_{80}Te_{20})_{96}Ag_4$	I	40.9850	2.39	2	40.9850	88.735	44.3675
	II	45.3341	2.44	2	45.3341	103.661	51.8305

According to Matusita et. al. [14]

$$\ln[-\ln(1-X_c)] = -n\ln\beta - \frac{1.052mE_c}{RT_p}$$

where X_c is the volume fraction of crystals precipitated in the glass heated at a uniform rate, E_c is the activation energy for crystallization. The slope of $\ln[-\ln(1-X_c)]$ vs. lnβ (Fig. 11) gives the value of n for first and second phase respectively shown in Table 2. The slope of the straight lines in $\ln[-\ln(1-X_{c1})]$ vs. 1000/T (Fig. 12) and $\ln[-\ln(1-X_{c2})]$ vs. 1000/T (Fig. 13) plots gives the value of mE_c for both phases listed in Table 2.

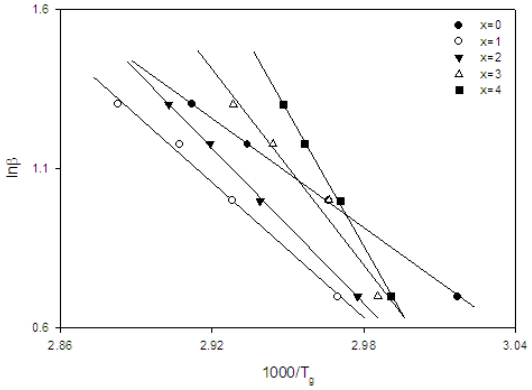

Fig. 8 Plot of lnβ vs $1000/T_g$ for $(Se_{80}Te_{20})_{100-x}Ag_x$ glassy system.

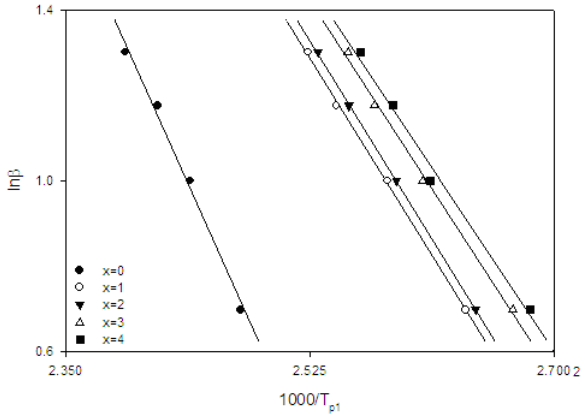

Fig. 9 Plot of logβ vs 1000/T_{p1} for $(Se_{80}Te_{20})_{100-x}Ag_x$ glassy system.

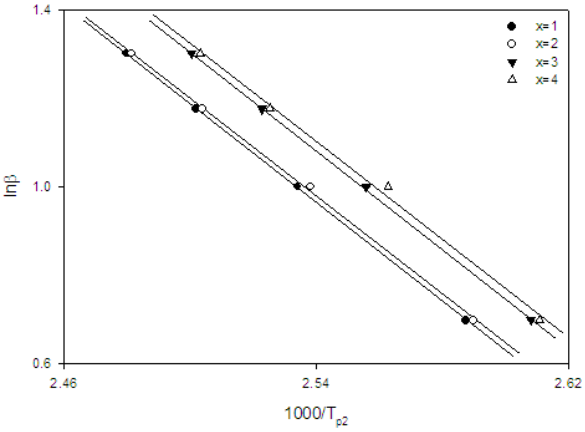

Fig. 10 Plot of logβ vs 1000/T_{p2} for $(Se_{80}Te_{20})_{100-x}Ag_x$ glassy system.

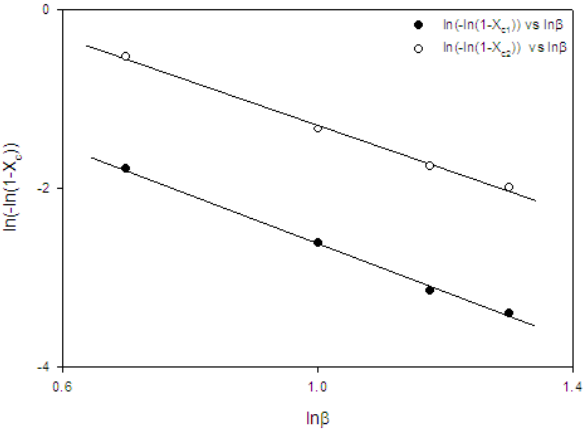

Fig. 11 The plot of ln[-ln(1-X_c)] vs lnβ for both exothermic peaks at different heating rates of sample for $(Se_{80}Te_{20})_{100-x}Ag_x$ (x=2) at 378K.

4. Discussion

Glassy Se has both chain as well as Se_8 ring structures [27]. Addition of Te leads to increase in the Se-Te mixed rings with simultaneous increase in Se and Te atoms in chain structure but there is decrease in the Se_8 ring concentrations. When Ag is incorporated, it makes bonds with Se and probably is dissolved in the Se chains. Thus there is decrease in the number of long Se-Te polymeric chains and Se-Te mixed rings but there is increase in the Se_8 rings. The decrease in chain length may be causing a decrease in T_g [28]. This reason explains the decrease in T_g with increase in Ag content. The slope of ln[-ln(1 – X_c)] vs. lnβ (Fig. 11) gives the value of n for first and second phase respectively. Mahadevan [29] has shown that n can take value 4,3,2,1 related to different types of glass crystal transformation mechanism. n=4 represents volume nucleation and three dimensional growth, n=3 represent volume nucleation and two dimensional growth, n=2 represents volume nucleation and one dimensional growth, n=1 represents surface nucleation and one dimensional growth from surface to inside. The value of m is taken as equal to n because the sample has undergone a heat treatment [30]. In the present case no heat treatment was given, however, the presence of an endothermic peak indicates that a thermal relaxation has taken place. Also, due to the lower value of the T_g, it can be reasonably assumed that the sample might have undergone a heat treatment at room temperature. Hence, the value of m is taken as equal to n in the present case for further analysis. The values of both m and n are reported in Table 2. Thus in the case of our samples, values of n=2 and m=2 reveal volume nucleation and one-dimensional growth. Using the values of n and m, the activation energy of crystallization E_c was calculated from both modified Kissinger and Matusita methods. The calculated values of E_c are given in Table 2 as E_c (MK), and E_c (ME) for modified Kissinger equation and Matusita equation respectively. Both show some discrepancy. This discrepancy in E_c may be due to the different approximations that have been adopted while arriving at the final equation of different formulae. Besides, the variability of location of the temperature measuring thermocouple may introduce error on temperature axis of a thermoanalytical curve. Similar discrepancy in other materials has also been reported [13, 31, 32]. The deviation from the straight-line nature at higher temperature is due to saturation of nucleation sites during the latter stage in the process of crystallization [23] or to the restriction of crystal growth by the small size of the particles [33]. Fig. 14 shows the crystallized fraction as a function of temperature for phase first phase (a) and second phase (b) at different heating rates. It has been found that there is increase in the fraction of crystallization with increase in the temperature.

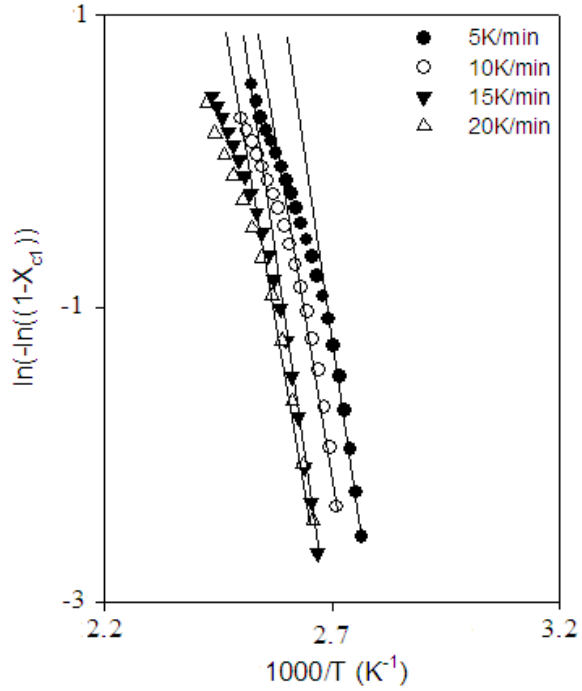

Fig. 12 Plot of ln[-ln(1-X_{c1})] vs 1000/T for first exothermic peak at different heating rates of $(Se_{80}Te_{20})_{98}Ag_2$ glassy system.

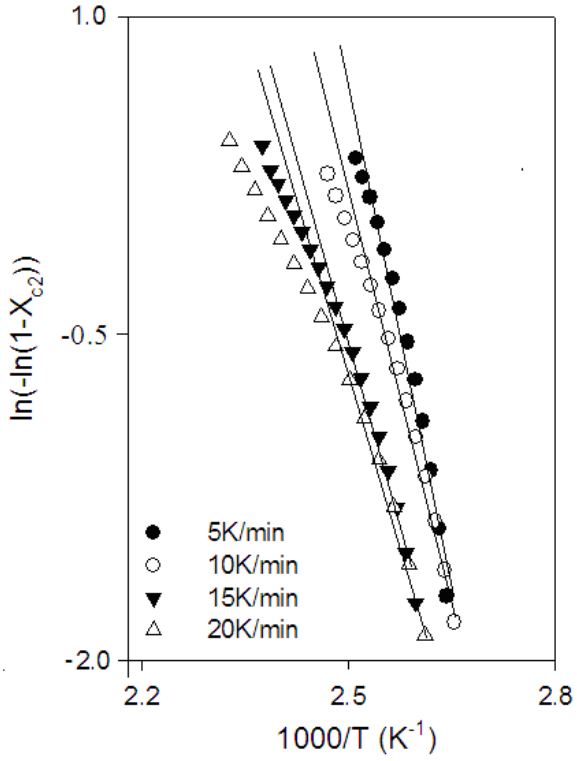

Fig. 13 Plot of ln[-ln(1-X_{c2})] vs 1000/T for second exothermic peak at different heating rates of $(Se_{80}Te_{20})_{98}Ag_2$ glassy system.

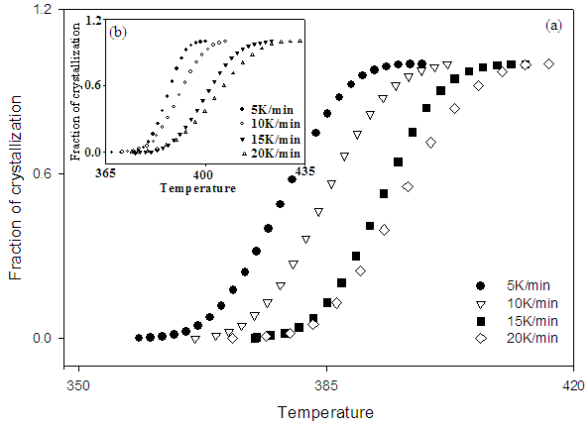

Fig. 14 Shows the increase of fraction of crystallization as the temperature increase with heating of sample for $(Se_{80}Te_{20})_{100-x}Ag_x$ (x=2) for first exothermic peak (a) and for second exothermic peak (b).

5. Conclusion

DSC studies have been performed on bulk $(Se_{80}Te_{20})_{100-x}Ag_x$ (x =0, 1, 2, 3 and 4) samples and the effect of addition of Ag to Se–Te system have been investigated. Both T_g and T_c decrease with increase in Ag concentration. The addition of Ag leads to formation of Ag–Se bonds and αAg_5Te_3 phase. The activation energy of crystallization has been determined by using Modified Kissinger equation and Matusita equation. On comparison of the values of E_c obtained from these two relations, some discrepancy has been found.

References

[1] E. Maruyama, Jpn. J. Appl. Phys. **21**, 231 (1982).
[2] D. C Hunt, S. S. Kirby, J. A. Rowlands, Med. Phys. **29**, 2464 (2002).
[3] T. Wagnar, S. O. Kasap, J. Mater. Res. **12**, 1892 (1997).
[4] K. Tanaka, Phys. Rev. B **39**, 1270 (1989).
[5] K. Shimakawa, J. Non-Cryst. Solids **77–78**, 1253 (1985).
[6] J. Y. Shim, S. W. Park, H. K. Baik, Thin Solid Films **292**, 31 (1997).
[7] J. M. Saitar, J. Ledru, A. Hamou, G. Saffarini, Physica B **245**, 256 (1998).
[8] R. Chiba, N. Funakoshi, J. Non-Cryst. Solids **105**, 149 (1988).
[9] A. Bhargava, A. Williamson, Y. K. Vijay, I. P. Jain, J. Non-Cryst. Solids **192**, 494 (1995).
[10] R. M. Mehra, G. Kaur, A. Pundir, P. C. Mathur, Jpn. J. Appl. Phys. **32**, 128 (1993).
[11] Z. Wang, C. Tu, Y. LI, Q. Chen, J. Non-Cryst. Solids **191**, 132 (1995).
[12] S. O. Kasap, T. Wagner, V. Aiyah, O. Krylouk, A. Bekirov, L. Tichy, J. Mat. Sci. **34**, 3779 (1999).

[13] M. S. Kamboj, R. Thangaraj, Eur. Phys. J. Appl. Phys. **24**, 33 (2003).
[14] K. Matusita, T. Komatsu, R. Yokota, J. Mater. Sci. **19**, 291 (1984).
[15] J. Vazquez, P. L. Lopez-Alemany, P. Villares, R. Jimenez-Garay, J. Phys. Chem. Solids **61**, 493 (2000).
[16] M. J. Strink, A. M. Zahra, Thermochima Acta **298**, 179 (1997).
[17] F. C. Kracek, C. J. Ksanda, The American Mineralogist **51**, 14 (1966).
[18] V. Simic, Z. Marinkovic, J. Mater. Sci. **33**, 561 (1998).
[19] M. Lasoka, Mat. Sci. Eng. **23**, 173 (1976).
[20] S. O. Kasap, C. Juhaz, J. Mater. Sci. 24, 1329 (1986).
[21] J. P. Larmagnac, J. Grenet, P. Michon, J. Non- Cryst. Solids **45**, 157 (1981).
[22] C. T. Moynihan, A. J. Easteal, J. Wilder, J. Tucker, J. Phys. Chem. **78,** 267 (1974).
[23] J. Colemenero, J. M. Barabdiaran, J. Non-Cryst Solids **30**, 263 (1979)
[24] J.E. Shelby, J. Non-Cryst Solids **34**, 111 (1979)
[25] K. Matusita, S. Saka, Phys. Chem. Glasses **20**, 81 (1979)
[26] D. R. Macfarane, M. Maecki, M. Paulain, J. Non-Cryst. Solids. **64**, 351 (1984)
[27] J. Schottmiller, M. Tabac, G. Lucovsky, A. Ward, J. Non-Cryst Solids **4**, 80 (1970)
[28] A. Eisenberg, Polym. Lett. **1**, 177 (1963)
[29] S. Mahadevan, A. Giridhar, A. K. Singh, J. Non-Cryst. Solids **88**, 11 (1986)
[30] P. Agarwal, S. Goel, J. S. P. Rai, A. Kumar, Phys. Status Solidi a **127**, 363 (1991).
[31] G. Kaur, T. Komatsu, R. Thangaraj, J. Mater. Sci. **35**, 903 (2000)
[32] G. Kaur, T. Komatsu, J. Mater. Sci. **36**, 4531 (2001)
[33] R. F Speyer, S. H. Risbud, Phys. Chem. Glasses **24,** 26 (1983)

*Corresponding author: rthangaraj@rediffmail.com